Catalysis Today 158 (2010) 432–438

Contents lists available at ScienceDirect

Catalysis Today

journal homepage: www.elsevier.com/locate/cattod

NO_x storage and reduction performance of Pt–CoO_x–BaO/Al_2O_3 catalysts: Effects of cobalt loading and calcination temperature

Zhun Hu, Ke-Qiang Sun*, Wei-Zhen Li, Bo-Qing Xu*

Innovative Catalysis Program, Key Lab of Organic Optoelectronics and Molecular Engineering, Department of Chemistry, Tsinghua University, 100084 Beijing, Haidian District, China

ARTICLE INFO

Article history:
Available online 14 July 2010

Keywords:
NO_x storage and reduction
Pt–BaO catalysts
Cobalt oxides
N_2 selectivity
Binary Pt–Co oxides

ABSTRACT

The NO_x storage and reduction (NSR) performance of low platinum (0.5 wt%) 0.5Pt–CoO_x–15BaO/Al_2O_3 catalysts with varied Co loadings and calcination temperatures was studied to investigate the promotional effect of CoO_x on the NSR catalysis. The NSR performance was tested under cyclic lean–rich conditions, and was evaluated in terms of NO_x storage capacity (NSC) under the lean condition, the N_2 selectivity and the amount of nitrogen-containing products (namely, the NO_x reduction capacity (NRC)) under the rich condition. For the catalysts calcined at 800 °C, addition of CoO_x to the 0.5Pt–15BaO/Al_2O_3 catalyst enhanced the NSC but lowered significantly the NRC, which made the NRC/NSC ratios dropped significantly from 0.82 for the reference 0.5Pt–15BaO/Al_2O_3 catalyst to around 0.50 for the catalysts containing 1 and 5 wt% Co, and to 0.37 for the catalyst containing 10 wt% Co. Moreover, the N_2 selectivity remained at around 50% for the 0.5Pt–CoO_x–15BaO/Al_2O_3 catalysts when the Co loading was kept low (0–5 wt%), and decreased significantly to 30% when the Co loading was 10 wt%. The calcination temperature of the 0.5Pt–CoO_x–15BaO/Al_2O_3 sample containing 5 wt% Co was varied in the range of 350–800 °C to improve the NSR performance. The catalyst calcined at 550 °C was found to produce the highest NRC/NSC ratio (0.80) and N_2 selectivity (76.1%) under the rich condition. The maximum efficiency for NSR catalysis of this catalyst seemed to be associated with the amount of binary Pt–Co oxides.

© 2010 Elsevier B.V. All rights reserved.

1. Introduction

Automobile lean-burn engines can improve fuel efficiency by ca. 20–30% over the traditional stoichiometric engines. However, the lean NO_x abatement, reducing NO_x to N_2 in the oxygen rich lean-exhausts represents a major technique challenge to control emission from the fuel efficient automobile. The catalytic NO_x storage and reduction (NSR) or lean NO_x trap (LNT) technology, proposed by Toyota researchers in the middle of 1990s [1,2], has been recognized as one of the most promising approaches to the lean NO_x abatement. The principle of NSR technology is based on the oxidative storage of NO_x primarily as nitrates over a NSR catalyst under the normal lean-burn operation (lean storage phase), followed by the reduction of the stored NO_x to N_2 under intermittently short rich-burn operation (rich regeneration phase) to recover the catalyst for NO_x storage. The NSR concept obviates the difficulty in selective reduction of NO_x under far excessive oxygen, but still preserves the fuel efficiency of the lean-burn engine since the lean storage phase is much longer than the rich regeneration phase.

The most investigated NSR catalyst system is based on Pt–BaO/Al_2O_3 consisting primarily of Pt and BaO dispersed on a γ-Al_2O_3 support. The basic BaO provides the NO_x storage sites and the Pt metal provides the active sites for the oxidation of NO during lean conditions as well as the reduction of the stored NO_x during rich conditions [3,4]. Extensive studies have been carried out to identify highly performing NSR catalysts. Addition of transition metal oxides (MnO_x, FeO_x, CeO_x, CoO_x) to Pt–BaO/Al_2O_3 was shown to be an effective way to improve the NO_x storage capacity (NSC) and the stability of the catalyst [5–12]. Of particular interest is the CoO_x promotion, it was found that an addition of 5 wt% Co enhanced the NSC of the conventional 1Pt–15BaO/Al_2O_3 catalyst (Pt and Ba loadings are 1 and 15 wt%, respectively) by 100% [7]. Particularly, a Co-promoted Pt–BaO/Al_2O_3 catalyst loaded as low as 0.25 wt% Pt produced a NSC comparable to the conventional 1Pt–15BaO/Al_2O_3 catalyst [7]. These findings suggest a promising way for reducing the cost of NSR catalysts by using in-expensive transition metal oxides to partially replace the expensive platinum group metals. However, these earlier studies were mainly directed to understand the NO_x storage performance under lean conditions, with less attention paid to the NO_x reduction under rich conditions. Recent research focused on understanding the reduction of the stored NO_x over the Pt–BaO/Al_2O_3 catalyst under rich conditions detected, in addition to N_2, the formation of undesired products such as NH_3

* Corresponding authors. Tel.: +86 10 62789022; fax: +86 10 62789022.
E-mail addresses: kqsun@mail.tsinghua.edu.cn (K.-Q. Sun), bqxu@mail.tsinghua.edu.cn (B.-Q. Xu).

0920-5861/$ – see front matter © 2010 Elsevier B.V. All rights reserved.
doi:10.1016/j.cattod.2010.06.008

and N_2O [13–16]. However, knowledge about the effect of CoO_x on the overall NSR performance especially on the reduction of the stored NO_x over Pt–CoO_x–BaO/Al_2O_3 catalyst is very limited.

In this work, we firstly investigated the characteristics of the NSR performance of low platinum (ca. 0.5 wt%) Pt–CoO_x–BaO/Al_2O_3 catalysts by varying the Co loading from 1 to 10 wt% but fixing the catalyst calcination at 800 °C. The catalyst calcination temperature was then changed in the range of 350–800 °C to understand the calcination temperature effect on the catalyst performance. Our evaluation of the NSR performance was made by paying particular attention to detecting every possible nitrogen-containing gas including NH_3 and N_2O under rich condition.

2. Experimental

2.1. Catalyst preparation

The γ-Al_2O_3 support (S_{BET} = 160 m^2/g, pore volume V_p = 0.37 cm^3/g) was prepared through conventional hydrolysis of $Al(NO_3)_3{\cdot}9H_2O$ with an aqueous ammonia solution at pH = 10. The obtained $Al(OH)_3$ hydrogel was then thoroughly washed, dried overnight at 110 °C and calcined in a flowing air at 800 °C for 5 h.

Pt–CoO_x–BaO/Al_2O_3 catalysts, with 0.5 wt% Pt and 15 wt% Ba were prepared via a sequential two-step wet impregnation method [17]. In the first step, BaO/Al_2O_3 sample was prepared by wet impregnation of the γ-Al_2O_3 with an aqueous solution of $Ba(NO_3)_2$, followed by drying at 60 °C in a rotary evaporator and calcination in a flowing air at 800 °C for 5 h. In the second step, Pt and Co were loaded by co-impregnation of the BaO/Al_2O_3 sample with an aqueous solution of $Pt(NH_3)_4(NO_3)_2$ (Alfa) and $Co(NO_3)_2{\cdot}6H_2O$, followed by drying at 60 °C in a rotary evaporator and calcination in a flowing air at 350–800 °C for 5 h. The composition of these catalysts was analyzed by XRF (Table 1). The catalysts thus prepared were denoted as 0.5Pt–*n*CoO_x–BaO/Al_2O_3-*T*, where "*n*" represented the Co loading and "*T*" the calcination temperature. Pt–BaO/Al_2O_3 with 0.5 wt% Pt and 15 wt% Ba was also prepared as a reference catalyst by the above procedure except that only Pt in the second step was loaded.

2.2. Characterization

X-ray diffraction (XRD) patterns were collected on a Bruker D8 Advance X-ray diffractometer with a Ni-filtered Cu K_α (λ = 0.15406 nm) radiation source at 40 kV and 40 mA.

Temperature programmed reduction (TPR) experiments were conducted in a flow of 5 vol% H_2 in Ar on a home-made TPR equipment with a TCD detector as described previously [17,18]. About 50 mg of catalyst was placed in a quartz reactor (4 mm i.d.) and pretreated with pure oxygen at the catalyst calcination temperature for 30 min and then cooled down to room temperature. After stabilization of the baseline in a flow of 5 vol% H_2 in Ar, the temperature was then raised to 800 °C with a temperature ramp of 10 °C/min and held at the final temperature for 30 min. Water formed during the reduction was completely removed with a cold trap (−100 °C) to avoid its interference to the TCD signal.

Table 1
Composition of 0.5Pt–*n*CoO_x–15BaO/Al_2O_3 catalysts.

Catalyst	Loading[a] (wt%)		
	Pt	Ba	Co
0.5Pt–15BaO/Al_2O_3-800	0.46	15.4	–
0.5Pt–1CoO_x–15BaO/Al_2O_3-800	0.46	15.3	0.98
0.5Pt–5CoO_x–15BaO/Al_2O_3-*T*[b]	0.44	15.2	4.91
0.5Pt–10CoO_x–15BaO/Al_2O_3-800	0.47	15.5	9.94

[a] Determined by XRF.
[b] "*T*" represents the calcination temperature of 350, 450, 550, 650 and 800 °C, respectively.

2.3. Evaluation of NSR performance

The NO_x storage and reduction performance of the catalysts was evaluated using a fixed bed plug-flow quartz reactor (4 mm i.d.) under cyclic lean (1000 ppm NO and 10 vol% O_2 in Ar, 50 min) and rich (1 vol% H_2 in Ar, 15 min) conditions at 300 °C. The lean–rich switches were intervened by an Ar purge for 5 min, which removes those NO_x reversibly adsorbed on the catalyst and flushes gaseous NO_x in the reactor tube, and thus is helpful for studying the intrinsic performance of the catalysts for the reduction of the stored NO_x. Prior to each test, the catalyst (60 mg) was pretreated at its calcination temperature for 30 min in 5 vol% H_2 in Ar and subsequently cooled to 300 °C. The NSR data were collected under cycle-average steady state which was generally achieved after the second or third lean–rich cycle. The overall gas flow rate was 40 mL/min, which corresponds to a gas hourly space velocity of 40,000 mL/(g h). The reactor effluent was on-line analyzed by a well-calibrated mass spectrometer (Inprocess Instruments, GAM 200) with the following mass-to-charge (*m*/*e*) ratios: 2 (H_2), 15 (NH_3), 28 (N_2), 30 (NO, NO_2), 32 (O_2), 40 (Ar), 44 (N_2O) and 46 (NO_2). The time-averaged product selectivity under the rich condition was calculated based on the number of nitrogen atom in the nitrogen-containing products.

Temperature programmed desorption of NO_x (NO_x-TPD) experiment was conducted on the same setup for the NSR measurements in an Ar flow (40 mL/min) from 200 to 800 °C with a temperature ramp of 10 °C/min. Prior to the NO_x-TPD measurement, the sample was conditioned under the cyclic lean–rich conditions to reach a steady state, and then saturated with NO_x under the lean condition at 300 °C.

3. Results and discussion

3.1. Effect of cobalt loading

A series of 0.5Pt–*n*CoO_x–15BaO/Al_2O_3-800 catalysts with Co loadings varying from 1 to 10 wt% were used to investigate the effect of Co loading on the NSR performance. The XRD patterns of these catalysts as well as the Co-free reference 0.5Pt–15BaO/Al_2O_3-800 catalyst are shown in Fig. 1. All of the catalysts showed the peaks characteristic of γ-Al_2O_3 phase at 2θ = 19.5°, 31.6°, 32.7°, 37.5°, 39.5° and 45.7° (JCPDS 10-0425), of $BaAl_2O_4$ at 2θ = 19.6°, 28.3°, 34.3°, 40.1° and 41.0° (JCPDS 17-0306), and of metallic Pt at 2θ = 39.8° (JCPDS 04-0802). The diffractions at 2θ = 31.3°, 36.9° and 44.8° are characteristic of Co_3O_4, and their intensity increased with increasing the Co loading.

Fig. 2 shows the time-course of NO_x storage under the lean condition (breakthrough curve) over the 0.5Pt–*n*CoO_x–15BaO/Al_2O_3-800 catalysts. Complete NO_x uptake occurred upon exposing these catalysts to NO/O_2 mixture. After a short dead time, NO and NO_2 evolved simultaneously. The concentration of NO_x ($NO + NO_2$) then increased steadily, and after about 25 min, the outlet NO_x concentration reached that of the inlet NO, indicating that the catalyst was saturated. It is noted that the addition of CoO_x prolonged the dead time for the complete NO_x trapping and made the NO curves less prominent and the NO_2 curves more prominent compared with the reference 0.5Pt–15BaO/Al_2O_3-800 catalyst.

Quantified results for the NO_x storage are shown in Table 2. The NSC increased from 0.22 mmol/g for the reference catalyst (0.5Pt–15BaO/Al_2O_3-800) to 0.24 and 0.25 mmol/g for the catalysts loaded with 1 and 5 wt% Co (0.5Pt–1CoO_x–15BaO/Al_2O_3-800 and 0.5Pt–5CoO_x–15BaO/Al_2O_3-800), respectively, and then

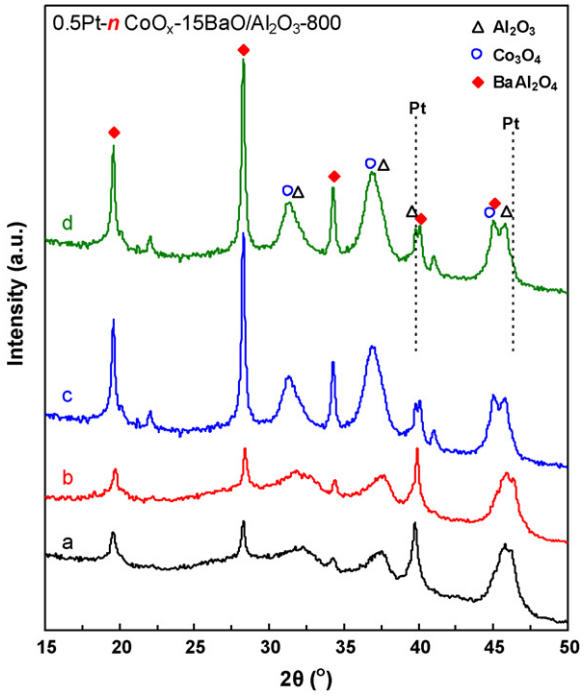

Fig. 1. XRD patterns of 0.5Pt–nCoO$_x$–15BaO/Al$_2$O$_3$-800 catalysts of n = 0 (a), 1 (b), 5 (c), 10 (d). The remarks refer to the diffraction peaks for Pt (dashed), Al$_2$O$_3$ (Δ), Co$_3$O$_4$ (○), BaAl$_2$O$_4$ (♦).

to 0.41 mmol/g when the Co loading was increased to 10 wt% (0.5Pt–10CoO$_x$–15BaO/Al$_2$O$_3$-800). The oxidation ability of these catalysts, evaluating by the NO$_2$/NO$_x$ ratio (Table 2) after being saturated with NO$_x$, also increased from 0.38 for the reference 0.5Pt–15BaO/Al$_2$O$_3$-800 to 0.43, 0.75 and 0.93 for the 0.5Pt–nCoO$_x$–15BaO/Al$_2$O$_3$-800 catalysts containing 1, 5 and 10 wt% Co, respectively. These results indicate that the oxidation activity of the catalyst increased significantly with the increasing Co loading, which are in line with the literature that additional catalytic sites for NO oxidation were generated due to the presence of CoO$_x$ (most probably in a form of Co$_3$O$_4$) [8,11].

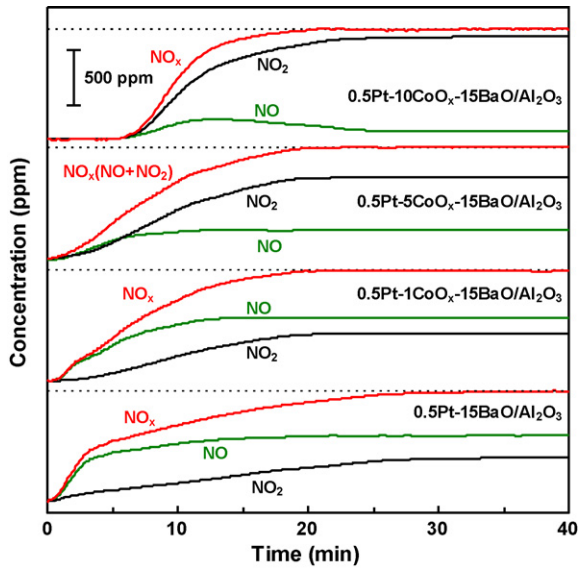

Fig. 2. Time-course of NO$_x$ storage under the lean condition (breakthrough curve) over 0.5Pt–nCoO$_x$–15BaO/Al$_2$O$_3$-800 catalysts with cobalt loading (n) of 0, 1, 5 and 10 wt%, respectively.

The different shapes of the breakthrough curves reflect the different intrinsic kinetics during NO$_x$ storage. Two main mechanisms have been proposed for NO$_x$ storage starting from "NO + O$_2$" [3,4]: the "nitrite route" – NO is oxidatively adsorbed as nitrites on neighboring Pt–BaO sites, followed by successive oxidation of the nitrites to nitrates; and the "nitrate route" – NO is oxidized to NO$_2$ on Pt sites followed by surface spillover or gas-phase diffusion to the "BaO" sites, and then stored as nitrates. In the second mechanism, one "BaO" site would react with three NO$_2$ molecules but only two of them can be stored, the other NO$_2$ molecule returned to NO via disproportionation (BaO + 3NO$_2$ → Ba(NO$_3$)$_2$ + NO). Therefore, the less prominent NO but more prominent NO$_2$ curves after the addition of CoO$_x$ to the 0.5Pt–15BaO/Al$_2$O$_3$-800 catalyst would indicate that the presence of CoO$_x$ depressed the disproportionation reaction of NO$_2$ and would therefore imply that the "nitrite route" prevails on the Co-containing catalysts. This explanation is in line with the literature that CoO$_x$ could provide additional boundary for NO$_x$ and oxygen spillover to BaO [8,11].

Fig. 3 shows the time-course of NO$_x$ reduction under the rich condition over the 0.5Pt–nCoO$_x$–15BaO/Al$_2$O$_3$-800 catalysts of varied Co loadings. N$_2$ was detected immediately upon exposure of the stored NO$_x$ to the flowing 1 vol% H$_2$/Ar and its concentration reached a plateau in less than 1 min, during which complete consumption of H$_2$ was observed. For the reference 0.5Pt–15BaO/Al$_2$O$_3$-800, the plateau concentration of N$_2$ was about 2000 ppm, which agrees well with that expected from the stoichiometry of nitrates reduction with H$_2$ ($2NO_3^- + 5H_2 \rightarrow N_2 + O^{2-} + 5H_2O$), suggesting that the reduction of the stored NO$_x$ is very fast and limited by the supply of H$_2$. However, adding 1 wt% Co to the 0.5Pt–15BaO/Al$_2$O$_3$-800 catalyst lowered significantly the plateau N$_2$ concentration. And, such a lowering in the N$_2$ plateau concentration became more pronounced with increasing the Co loading. In addition to the N$_2$ formation, NH$_3$, N$_2$O, and even NO and NO$_2$ were also detected in concentrations dependent on the Co loading. For the 0.5Pt–nCoO$_x$–15BaO/Al$_2$O$_3$-800 catalysts with $n \leq 5$ (including the reference catalyst), the formation of N$_2$ dominated clearly over the other products (N$_2$O, NO and NO$_2$) in the first minute or so, and the formation of NH$_3$ coincided basically with the evolution of unreacted H$_2$. The change of the reduction product selectivity to favor NH$_3$ formation after the N$_2$ peak was in good agreement with the literature [13–17]. However, for the 0.5Pt–10CoO$_x$–15BaO/Al$_2$O$_3$-800 catalyst with n = 10, N$_2$ and NH$_3$, and also the other products (N$_2$O, NO and NO$_2$) were simultaneously produced even at the very initial moments of the H$_2$ admission.

Quantified results for the overall reduction of the stored NO$_x$ under the rich condition are presented in Table 2. The product selectivity on the 0.5Pt–nCoO$_x$–15BaO/Al$_2$O$_3$-800 catalysts with Co loadings no higher than 5 wt% is quite similar, showing N$_2$ selectivity of around 50%. For the 0.5Pt–10CoO$_x$–15BaO/Al$_2$O$_3$-800 catalyst, however, the N$_2$ selectivity decreased to as low as 30%, while the respective selectivity to N$_2$O and NO$_x$ increased to as high as ca. 25%.

The most striking effect of CoO$_x$ addition to the Pt–BaO catalyst was exemplified by the amount of nitrogen-containing products detected under the rich condition, namely the NO$_x$ reduction capacity (NRC). The NRC decreased from 0.18 mmol/g for the reference 0.5Pt–15BaO/Al$_2$O$_3$-800 catalyst to 0.12, 0.14 and 0.15 mmol/g for the 0.5Pt–nCoO$_x$–15BaO/Al$_2$O$_3$-800 catalysts with n = 1, 5 and 10, respectively. This observation contrasts sharply with the enhanced NSC measured under the lean condition on cobalt addition. To highlight the different effects of CoO$_x$ on the NSC and the NRC, NRC/NSC ratios were then calculated. The NRC/NSC ratio (Table 2) was 0.82 for the reference 0.5Pt–15BaO/Al$_2$O$_3$-800 catalyst, but dropped significantly to around 0.50 for the 0.5Pt–nCoO$_x$–15BaO/Al$_2$O$_3$-800 catalysts containing 1% and 5 wt% Co, and further to 0.37 for the 0.5Pt–10CoO$_x$–15BaO/Al$_2$O$_3$-800 catalyst.

Table 2
NO_x storage and reduction performance of 0.5Pt–$n$$CoO_x$–15BaO/$Al_2O_3$-800 catalysts measured under lean (1000 ppm NO, 10% O_2 in Ar)/rich (1% H_2 in Ar) conditions.

Catalyst	NO_x storage		NO_x reduction						NRC/NSC
	NSC[a]	NO_2/NO_x[b]	NRC[c]	Selectivity[d] (N%)					
				N_2	NH_3	N_2O	NO	NO_2	
0.5Pt–BaO/Al_2O_3	0.22	0.38	0.18	52.5	38.3	9.2	0.0	0.0	0.82
0.5Pt–1CoO_x–BaO/Al_2O_3	0.24	0.43	0.12	49.2	45.0	5.8	0.0	0.0	0.50
0.5Pt–5CoO_x–BaO/Al_2O_3	0.25	0.75	0.14	51.3	39.5	4.9	4.3	0.0	0.56
0.5Pt–10CoO_x–BaO/Al_2O_3	0.41	0.93	0.15	29.8	19.7	24.2	23.4	2.9	0.37

[a] NO_x storage capacity (mmol/g-cat) based on nitrogen number under the lean condition.
[b] Fraction of NO_2 in the effluent NO_x when the catalysts were saturated by NO/O_2 adsorption.
[c] Amount of nitrogen-containing products (mmol/g-cat) based on nitrogen number detected under the rich condition.
[d] Time-averaged overall selectivity based on the nitrogen calibration.

The smaller numbers of NRC in comparison with their corresponding NSCs were caused by the removal of reversibly adsorbed NO_x during the Ar purge intervening the lean–rich switches. The significant drop in the NRC/NSC ratio after the Co addition indicates that the fraction of the reversibly adsorbed NO_x among the stored NO_x over the 0.5Pt–$n$$CoO_x$–15BaO/$Al_2O_3$-800 catalysts was much higher than that over the reference 0.5Pt–15BaO/Al_2O_3-800 catalyst. Noted that in the study when the lean-to-rich switch was not intervened by an inert gas purge, distinct "overshoot" of NO_x at the beginning of the reduction phase was observed on Co-containing catalysts by Vijay et al. [7]. The "overshoot" of NO_x was attributed to reversibly adsorbed NO_x, which would contribute to a larger NSC but virtually cannot be reduced to N_2. Therefore, the enhanced reversible adsorption of NO_x over the present 0.5Pt–$n$$CoO_x$–15BaO/$Al_2O_3$-800 catalysts, i.e., the smaller NRC/NSC ratios (≤0.56), implies that a large part of the NO_x under the lean phase cannot lead to NO_x abatement in the whole lean–rich cycle. Taking into account of the lower N_2 selectivity (Table 2), the above results strongly indicate that the addition of CoO_x to the reference low platinum catalyst 0.5Pt–15BaO/Al_2O_3-800 leads to severe performance deterioration of the NSR catalyst.

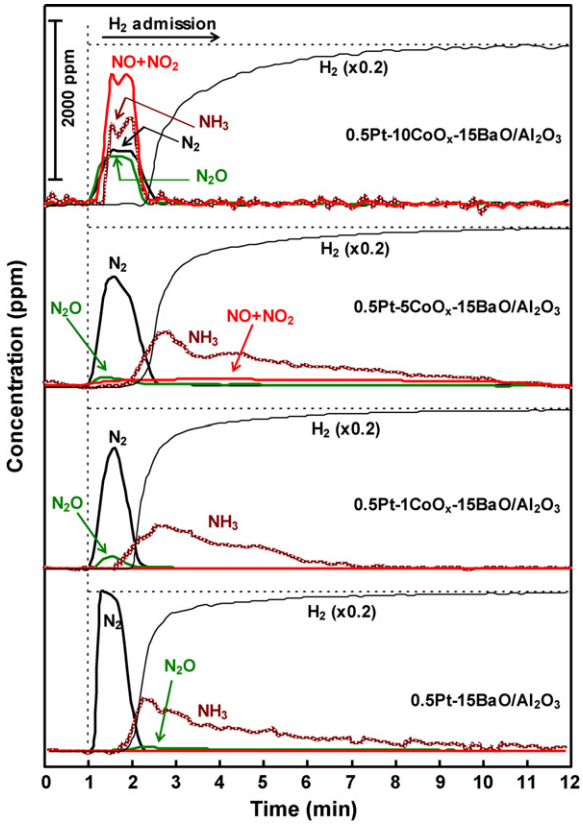

Fig. 3. Time-course of NO_x reduction under the rich condition over 0.5Pt–$n$$CoO_x$–15BaO/$Al_2O_3$-800 catalysts with cobalt loading (n) of 0, 1, 5 and 10 wt%, respectively.

The NSR performance of Pt–BaO catalyst depends critically on the nature of the BaO-based NO_x trapping sites (BaO), the Pt-based redox sites for NO_x oxidation and reduction catalysis, and the Pt–BaO interaction [3,4,19]. The 0.5Pt–$n$$CoO_x$–15BaO/$Al_2O_3$-800 catalysts investigated as above were prepared by the sequential two-step impregnation method. Before the loading of Pt and CoO_x (i.e., co-impregnation in the second step), the BaO sites were generated by calcination at 800 °C in the first step (i.e., impregnation of $Ba(NO_3)_2$). The added CoO_x could modify the Pt sites and Pt–BaO interaction, and also generate new CoO_x–BaO interaction. These factors would be likely responsible for the deterioration of the NSR performance after the Co addition. It was reported that the catalyst calcination temperature would affect significantly the nature of Pt–CoO_x interactions [20]. We therefore studied in the following section the effect of catalyst calcination temperature on the NSR performance using the sample loaded with 5 wt% Co.

3.2. Effect of calcination temperature

Fig. 4 shows the time-course of NO_x storage under the lean condition over 0.5Pt–5CoO_x–15BaO/Al_2O_3-T catalysts with calcination temperature (T) varied from 350 to 800 °C. Lowering the T from 800 to 350 °C obviously prolonged the dead time period, i.e., the complete trapping of NO_x lasted for longer times. Furthermore, the breakthrough curves became less steep on decreasing the catalyst calcination temperature, and the time required for the outlet NO_x concentration to reach the inlet value extended from 25 min at T = 800 °C to 30 min (T = 650 °C), 35 min (T = 550 °C) and 45 min (T = 350 and 450 °C, respectively). Accordingly, the NSC (Table 3) increased monotonously from 0.25 to 0.52, 0.71, 0.89 and 0.92 mmol/g, respectively, when the T was lowered from 800 to 650, 550, 450 and 350 °C. On the other hand, the NO_2/NO_x ratio (Table 3), increased slightly from 0.75 at T = 800 °C to 0.80 and 0.81 mmol/g at T = 650 and 550 °C, respectively, and then decreased obviously to 0.60 and 0.65 at T = 450 and 350 °C, respectively. These results indicated clearly that the NO_x storage performance of the 0.5Pt–5CoO_x–15BaO/Al_2O_3-T catalysts has been profoundly modified with the calcination temperature.

The performance of the 0.5Pt–5CoO_x–15BaO/Al_2O_3-T catalysts for the reduction of the stored NO_x is shown in Fig. 5 by presenting the time-course of NO_x reduction under the rich condition. The evolution profiles over these catalysts were similar, characterized by the dominate formation of N_2 in the first minute or so, and the subsequent formation of NH_3 coincided with the evolution of unreacted H_2 when the stored NO_x was largely consumed. Furthermore, traces of N_2O and NO_x (NO + NO_2) were detected over the catalyst

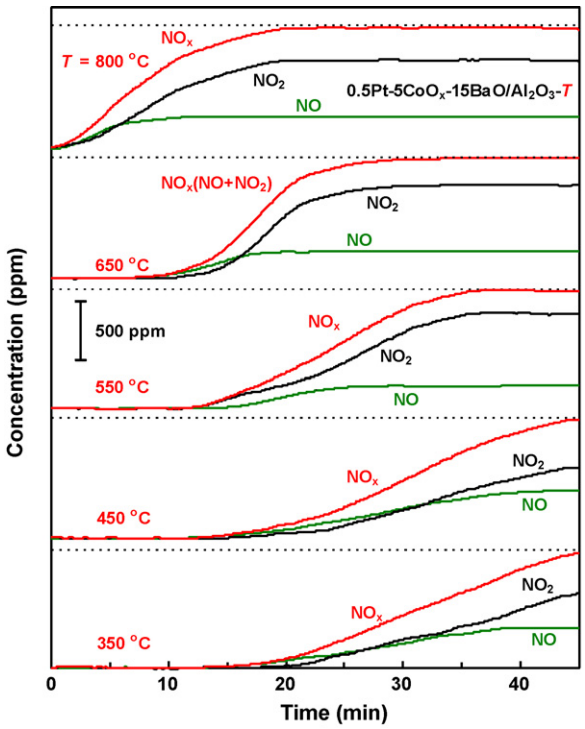

Fig. 4. Time-course of NO_x storage under the lean condition (breakthrough curve) over 0.5Pt–5CoO_x–15BaO/Al_2O_3-*T* catalysts with calcination temperature (*T*) of 350, 450, 550, 650 and 800 °C, respectively.

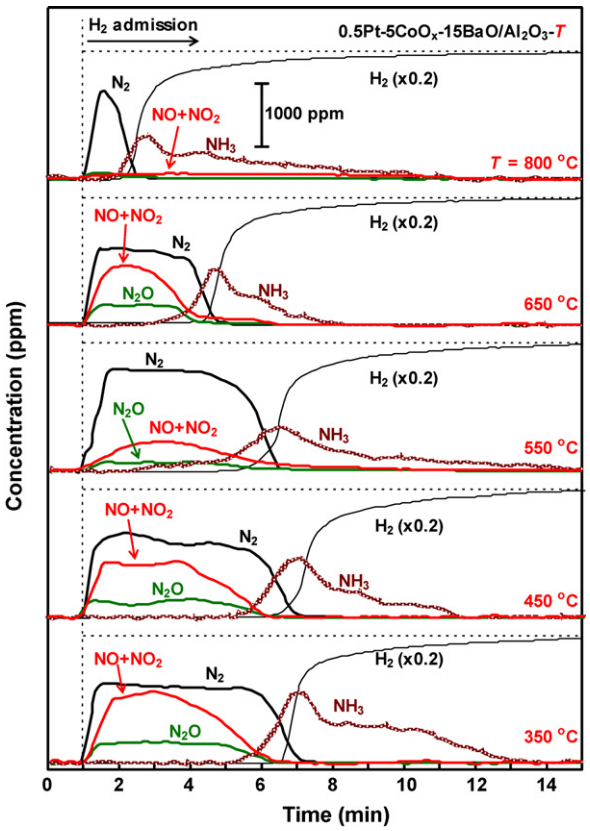

Fig. 5. Time-course of NO_x reduction under the rich condition over 0.5Pt–5CoO_x–15BaO/Al_2O_3-*T* catalysts with calcination temperature (*T*) of 350, 450, 550, 650 and 800 °C, respectively.

of *T* = 800 °C, but their production was much more pronounced for the catalysts of *T* < 800 °C.

Quantified results for the reduction of the stored NO_x over the 0.5Pt–5CoO_x–15BaO/Al_2O_3-*T* catalysts are shown in Table 3. The N_2 selectivity increased remarkably from 51.3% to 76.1% when the *T* was lowered from 800 to 550 °C. However, the N_2 selectivity then decreased to around 60% on further lowering the *T* to 450 and 350 °C. The selectivity of the other products (NH_3, N_2O, NO and NO_2) also depends markedly on the calcination temperature. The NH_3 selectivity dropped from 39.5% for the catalyst of *T* = 800 °C to below 15% for the catalysts of *T* < 800 °C, while the overall selectivity to N_2O, NO and NO_2 increased from about 9% at *T* = 800 °C to above 15% for the catalysts of *T* < 800 °C. The measurement of NRC provides another criterion to evaluate the catalyst performance. Although the number of NRC increased monotonously with lowering the calcination temperature, the NRC/NSC ratio (Table 3) showed a maximum of 0.80 at *T* = 550 °C. These results clearly indicate that the catalyst of *T* = 550 °C showed the maximum efficiency for NSR catalysis. It should be noted that the N_2 selectivity of the 0.5Pt–5CoO_x–15BaO/Al_2O_3-550 catalyst was still substantially lower than that (84.8%) of the 0.5Pt–15BaO/ZrO_2–Al_2O_3 catalyst (0.5 wt% Pt) which we uncovered very recently [17], but much higher than that of the reference 0.5Pt–15BaO/Al_2O_3-800 catalyst. The above results indicate also that the clear detection of every possible nitrogen-containing product (N_2, NH_3, N_2O, NO and NO_2) during the reduction of the stored NO_x under the rich condition, is important for accurate evaluation of the actual deNO_x (to N_2) capability of NSR catalyst.

The product selectivity during the reduction of the stored NO_x depends intrinsically on the local ratio of the concentration of nitrogen-containing species to that of the hydrogen (N/H ratio) on the Pt sites where NO_x reduction occurs [13–16,19,21]. Higher N/H ratio would favor the formation of N_2, while the lower ratio the formation of NH_3. Since the activation of H_2 on Pt sites is not the limiting step, as indicated by the complete consumption of H_2 at the initial exposure of the stored NO_x to the flowing H_2/Ar

Table 3
NO_x storage and reduction performance of 0.5Pt–5CoO_x–15BaO/Al_2O_3 catalysts measured under lean (1000 ppm NO, 10% O_2 in Ar)/rich (1% H_2 in Ar) conditions.

Calc. temp.	NO_x storage		NO_x reduction						NRC/NSC
	NSC[a]	NO_2/NO_x[b]	NRC[c]	Selectivity[d] (N%)					
				N_2	NH_3	N_2O	NO	NO_2	
350	0.92	0.65	0.67	58.6	14.8	11.2	12.0	3.4	0.73
450	0.89	0.60	0.60	63.8	12.2	9.9	12.3	1.8	0.67
550	0.71	0.81	0.57	76.1	9.3	6.3	4.3	4.0	0.80
650	0.52	0.80	0.38	54.8	12.7	13.8	13.8	4.9	0.73
800	0.25	0.75	0.14	51.3	39.5	4.9	4.3	0.0	0.56

[a] NO_x storage capacity (mmol/g-cat) based on nitrogen number under the lean condition.
[b] Fraction of NO_2 in the effluent NO_x when the catalysts were saturated by NO/O_2 adsorption.
[c] Amount of nitrogen-containing products (mmol/g-cat) based on nitrogen number detected under the rich condition.
[d] Time-averaged overall selectivity based on the nitrogen calibration.

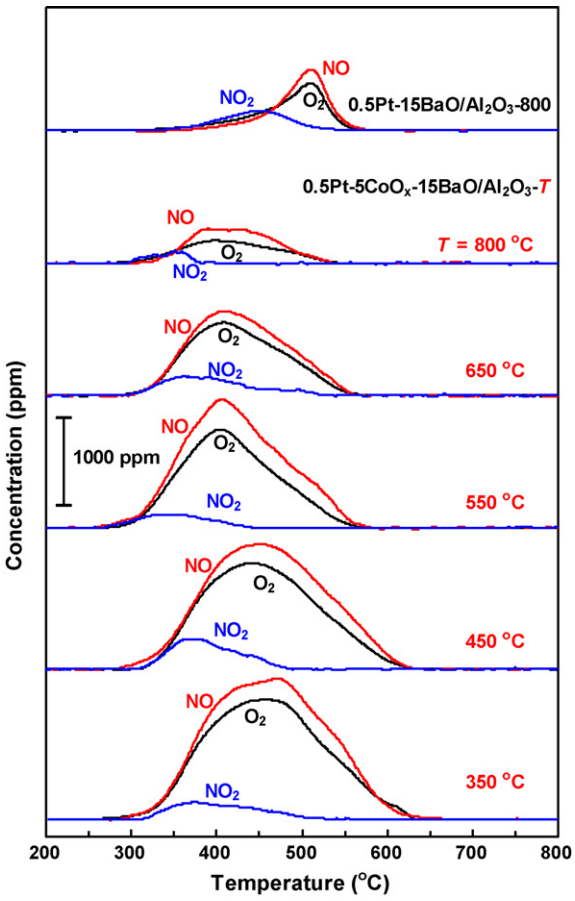

Fig. 6. NO_x-TPD profiles of 0.5Pt–15BaO/Al_2O_3-800 catalyst and 0.5Pt–5CoO_x–15BaO/Al_2O_3-*T* catalysts.

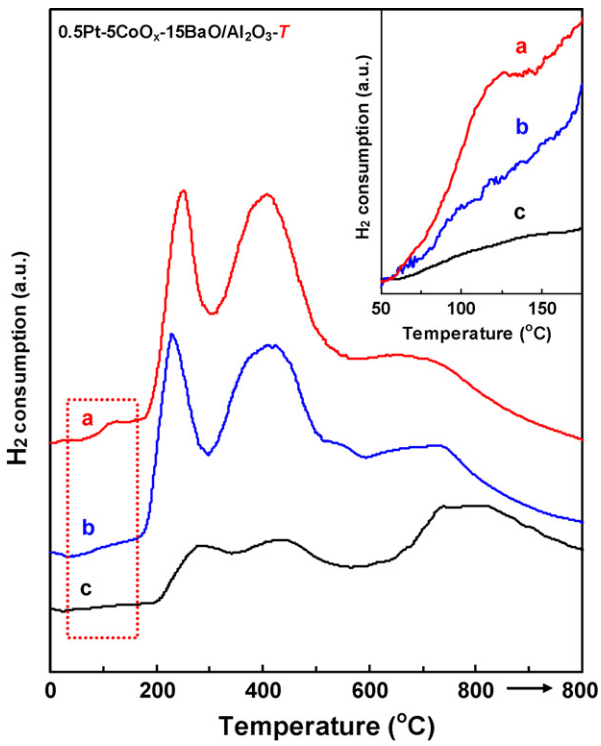

Fig. 7. H_2-TPR profiles of 0.5Pt–5CoO_x–15BaO/Al_2O_3-*T* catalysts of *T* = 550 °C (a), 650 °C (b) and 800 °C (c).

(Figs. 3 and 5), the release of NO_x from the tapping BaO sites is critical for the product selectivity.

The NO_x release performance of the 0.5Pt–5CoO_x–15BaO/Al_2O_3-*T* catalysts was then evaluated by NO_x-TPD after these catalysts had reached their steady states through lean–rich alternations and then saturated with NO_x under the lean condition at 300 °C. The NO_x-TPD curves (Fig. 6) of 0.5Pt–5CoO_x–15BaO/Al_2O_3-*T* catalysts were characterized by a broad NO peak in the temperature range of 300–600 °C, which enveloped a strong O_2 desorption peak and a very weak NO_2 peak. Compared to the distinct NO and NO_2 peaks observed on the NO_x-TPD curves of the reference 0.5Pt–15BaO/Al_2O_3-800 (Fig. 6) and of the 0.5Pt–15BaO/ZrO_2–Al_2O_3-800 reported in Ref. [17], the relative amount of desorbed NO_2 was significantly reduced and also the peaks of NO and NO_2 were shifted obviously to lower temperatures by the Co addition. It should be noted that the peak temperature for NO desorption was the lowest for the catalyst of *T* = 550 °C (0.5Pt–5CoO_x–15BaO/Al_2O_3-550). Remembering that this very catalyst produced the highest N_2 selectivity and the lowest NH_3 selectivity during NO_x reduction under the rich condition (Fig. 5 and Table 3), the above results suggest that the lower the desorption temperature of NO in NO_x-TPD, the higher the selectivity to N_2 during the reduction of the stored NO_x, which well supports our earlier observation made on ZrO_2–Al_2O_3 supported Pt–BaO catalysts [17].

The oxidative storage of NO_x on Pt–BaO catalyst is an equilibrium-driven reaction [3,4,22]. According to the principle of microreversibility, the NO_x release performance of the catalyst should be the integral result of many factors including the nature of different sites (BaO, Pt and CoO_x) as well as their interactions.

H_2-TPR profiles (Fig. 7) of 0.5Pt–5CoO_x–15BaO/Al_2O_3-*T* were then measured to gain information on the nature of Pt and CoO_x sites. The TPR profiles for the catalysts of *T* = 350 and 450 °C were not shown because the two catalysts contained nitrate salts of the precursor (e.g. $Co(NO_3)_2$, $Pt(NH_3)_4(NO_3)_2$). The reduction of these nitrates during the H_2-TPR experiment would produce various nitrogen-containing species that interfere strongly with the TCD signal. Three main reduction peaks in the temperature range of 190–320, 320–530 and 600–800 °C could be clearly identified on the TPR profiles of the catalysts of *T* = 550, 650 and 800 °C. The two peaks at lower temperatures were weakened simultaneously with increasing the catalyst calcination temperature (*T*). The intensity of the broad peak at 600–800 °C did not change obviously with the catalyst calcination temperature (*T*), but its maximum shifted from around 710 to 780 °C when the *T* was increased from 550 to 800 °C. The peaks at 190–320 and 320–530 °C were then assigned to the sequential reduction of Co^{3+} to Co^{2+} and Co^{2+} to metallic Co, respectively [23]. Note that the reduction of surface and bulk platinum oxides would also occur in these temperatures [24]. The broad peak at 600–800 °C could be assigned to the reduction associated with the Al_2O_3 support [17].

The TPR profile of the 0.5Pt–5CoO_x–15BaO/Al_2O_3-550 catalyst was characterized also by a small but distinctive peak at around 120 °C (insert of Fig. 7). Park et al. observed a similar peak at 100–130 °C on the TPR profiles of a series of Pt–Co/YSZ (YSZ: yttria-stabilized zirconia) catalysts differing in Co loading [20], which was assigned to the reduction of binary Pt–Co oxides, as discerned by careful HRTEM-EDX analysis [20]. Such binary Pt–Co oxides were of the most prominent on the Pt–Co/YSZ catalysts calcined at 500 °C but were converted to CoO_x covered Pt entities when the catalyst calcination temperature was raised to 700 °C [20]. The small but distinctive peak on the TPR profile of the 0.5Pt–5CoO_x–15BaO/Al_2O_3-550 catalyst could also be attributed to a formation of the binary Pt–Co oxides. It is therefore that the state of Pt and CoO_x, and their interaction in the present

0.5Pt–5CoO_x–15BaO/Al_2O_3-T catalysts were affected significantly by the calcination temperature T. The isolated and/or weakly interacted Pt and CoO_x entities were predominant on the catalysts of T = 350 and 450 °C. And, a part of these entities were converted at T = 550 °C to binary Pt–Co oxides, which further transformed to CoO_x covered Pt domains at T = 650 and 800 °C.

The 0.5Pt–5CoO_x–15BaO/Al_2O_3-550 catalyst exhibited the highest oxidation activity, as evidenced by the highest NO_2/NO_x ratio shown in Table 3, which could be due to the facile reduction of the Pt–Co binary oxides, since poisoning the Pt sites by strongly adsorbed oxygen was the main reason for the catalyst deactivation during NO oxidation [25]. The easier reduction of the Pt–Co binary oxides would also create a driving force for NO_x release from the trapping barium sites to Pt sites, which would account for the lowest NO_x desorption temperature in the NO_x-TPD profiles (Fig. 6) of the 0.5Pt–5CoO_x–15BaO/Al_2O_3-550 catalyst, and consequently the highest N_2 selectivity during the reduction of the stored NO_x under the rich condition (Fig. 5 and Table 3). Moreover, the presence of CoO_x–BaO boundary appeared to be detrimental to the NSR performance, as evidenced by the lowest NRC/NSC ratio (0.37) produced by the 0.5Pt–10CoO_x–15BaO/Al_2O_3-800 catalyst (10 wt% Co) (Table 2). The generation of the binary Pt–Co oxides on the catalyst of T = 550 °C would reduce the CoO_x–BaO boundary, as compared to the case of isolated CoO_x and Pt sites on the catalysts of T = 350 and 450 °C, and that of CoO_x covered Pt entities on the catalysts of T = 650 and 800 °C. Consequently, the 0.5Pt–5CoO_x–15BaO/Al_2O_3-550 characterized by the binary Pt–Co oxides produced the highest NRC/NSC ratio over the 0.5Pt–5CoO_x–15BaO/Al_2O_3-T catalysts. Further study would be required for understanding details of the composition and structure of the binary Pt–Co oxides in this highly performing NSR catalyst.

4. Conclusions

The present data agreed well with earlier literature that the promotion of conventional Pt–BaO/Al_2O_3 catalyst with CoO_x could lower the dependence on Pt of Pt–CoO_x–BaO/Al_2O_3 catalyst for the NO_x storage catalysis. The NSC of the 0.5Pt–CoO_x–15BaO/Al_2O_3-800 catalyst increased with the increment in the Co loading. On the other hand, the addition of CoO_x promoter lowered significantly the NRC/NSC ratio and produced no positive effect on the reduction of the stored NO_x under the rich condition when the Co loading was kept low (0–5 wt%) but very negative effect instead on further increasing the Co loading to 10 wt%, demonstrating that the presence of CoO_x was harmful to the NO_x reduction catalysis.

It was shown that the overall NSR performance of the 0.5Pt–5CoO_x–15BaO/Al_2O_3 (5 wt% Co) catalyst could be drastically affected by varying the catalyst calcination temperature in the range of 350–800 °C. The NRC/NSC ratio and the N_2 selectivity under the rich condition were maximized when the catalyst calcination was set at 550 °C. The maximum efficiency for NSR catalysis of this 0.5Pt–5CoO_x–15BaO/Al_2O_3-550 catalyst seemed to be associated with the amount of binary Pt–Co oxides. This work provided also clear detection of every possible nitrogen-containing product (N_2, NH_3, N_2O, NO and NO_2) during the reduction of the stored NO_x under the rich condition, which is important for accurate evaluation of the actual deNO_x (to N_2) capability of the NSR catalyst.

Acknowledgement

We thank National Natural Science Foundation of China (grants: 20703028 and 20921001) for the financial support of this work.

References

[1] N. Miyoshi, S. Matsumoto, K. Katoh, T. Tanaka, J. Harada, N. Takahashi, K. Yokota, M. Sugiura, K. Kasahara, SAE Technical Paper Series 950809, 1995.
[2] S. Matsumoto, Catal. Today 29 (1996) 43.
[3] W.S. Epling, L.E. Campbell, A. Yezerets, N.W. Currier, J.E. Parks, Catal. Rev. 46 (2004) 163.
[4] S. Roy, A. Baiker, Chem. Rev. 109 (2009) 4054.
[5] J.H. Xiao, H.X. Li, S. Deng, Catal. Commun. 9 (2008) 563.
[6] J.Y. Luo, M. Meng, Y.Q. Zha, Y.N. Xie, T.D. Hu, J. Zhang, T. Liu, Appl. Catal. B: Environ. 78 (2008) 38.
[7] R. Vijay, R.J. Hendershot, S.M. Rivera-Jimenez, W.B. Rogers, B.J. Feist, C.M. Snively, J. Lauterbach, Catal. Commun. 6 (2005) 167.
[8] R. Vijay, C.M. Snively, J. Lauterbach, J. Catal. 243 (2006) 368.
[9] J.H. Park, H.J. Cho, S.J. Park, I.S. Nam, G.K. Yeo, J.K. Kil, Y.K. Youn, Top. Catal. 42–43 (2007) 61.
[10] J.G. Kim, H.M. Lee, M.J. Lee, J.H. Lee, J.G. Kim, J.Y. Jeon, S.K. Jeong, S.J. Yoo, S.S. Kim, J. Ind. Eng. Chem. 14 (2008) 841.
[11] R. Vijay, H. Sakurai, C.M. Snively, J. Lauterbach, Top. Catal. 52 (2009) 1388.
[12] P.N. Lê, E.C. Corbos, X. Coutois, F. Can, S. Royer, P. Marecot, D. Duprez, Top. Catal. 52 (2009) 1771.
[13] L. Lietti, I. Nova, P. Forzatti, J. Catal. 257 (2008) 270.
[14] S.S. Mulla, S.S. Chaugule, A. Yezerets, N.W. Currier, W.N. Delgass, F.H. Ribeiro, Catal. Today 136 (2008) 136.
[15] I. Nova, L. Castoldi, L. Lietti, E. Tronconi, P. Forzatti, Top. Catal. 42–43 (2007) 21.
[16] W.S. Epling, A. Yezerets, N.W. Currier, Appl. Catal. B: Environ. 74 (2007) 117.
[17] W.-Z. Li, K.-Q. Sun, Z. Hu, B.-Q. Xu, Catal. Today (2010), doi:10.1016/j.cattod.2010.02.056.
[18] B.-Q. Xu, J.-M. Wei, H.-Y. Wang, K.-Q. Sun, Q.-M. Zhu, Catal. Today 68 (2001) 217.
[19] N.W. Cant, I. Liu, M.J. Patterson, J. Catal. 243 (2006) 309.
[20] E.Y. Ko, E.D. Park, H.C. Lee, D. Lee, S. Kim, Angew. Chem. Int. Ed. 46 (2007) 734.
[21] P. Forzatti, L. Lietti, I. Nova, Energy Environ. Sci. 1 (2008) 236.
[22] J. Coronado, J. Anderson, J. Mol. Catal. A: Chem. 138 (1999) 83.
[23] P. Arnoldy, J.A. Moulijn, J. Catal. 93 (1985) 38.
[24] C.P. Hwang, C.T. Yeh, J. Mol. Catal. A: Chem. 112 (1996) 295.
[25] L. Olsson, E. Fridell, J. Catal. 210 (2002) 340.